American Mineralogist, Volume 85, pages 570–577, 2000

Tetrahedral vacancies and cation ordering in low-temperature Mn-bearing vesuvianites: Indication of a hydrogarnet-like substitution

THOMAS ARMBRUSTER[1,*] AND EDWIN GNOS[2]

[1]Laboratorium für chemische und mineralogische Kristallographie, Universität Bern, Freiestrasse 3, CH-3012 Bern, Switzerland
[2]Mineralogisch-Petrographisches Institut, Universität Bern, Baltzerstrasse 1, CH-3012 Bern, Switzerland

ABSTRACT

Strongly zoned Mn-rich vesuvianites with MnO concentrations up to 14.3 wt% from the N'chwaning II mine of the Kalahari manganese field (South Africa) crystallized at hydrothermal conditions below 450 °C. These vesuvianites are by far the most Mn-rich samples hitherto described and have either space group *P*4*nc* or *P*4/*n* due to partial long-range ordering. Most crystals are assembled of *P*4*nc* and *P*4/*n* domains yielding *P*4 average symmetry. The crystal structure of one Mn-rich crystal of average composition $Ca_{19}Mn_{3.5}Al_{9.5}Si_{17.4}(O,OH)_{78}$ was refined from single-crystal X-ray data (R1 = 3.85%) in space group *P*4/*n* (*a* = 15.571(2), *c* = 11.789(2) Å). Mn^{2+} and Mn^{3+} are concentrated on the fivefold-coordinated square pyramidal Y' site. Additional Mn^{3+} was located on the octahedral sites Y2a (35%), Y1a (22%), Y2b (13%) and Y1b (8%). Electron microprobe analyses and crystal-structure refinements indicated tetrahedral vacancies in the orthosilicate tetrahedra (Z1 and Z2) but not in the disilicate units (Z3). Z1 tetrahedra with up to 17% vacancies have strongly increased Z1-O distances of 1.67 Å. Structural and chemical evidence combined with the similarity of the structures of vesuvianite and garnet suggest a partial hydrogarnet-like substitution of SiO_4 tetrahedra by H_4O_4.

INTRODUCTION

Vesuvianite is chemically and structurally one of the more complicated rock-forming minerals. It occurs in calc-silicate rocks equilibrated under a wide range of metamorphic pressures and temperatures but also in rodingites and altered alkaline rocks, e.g., nepheline syenites (Valley et al. 1985). An idealized formula may be written as $Ca_{19}Mg(MgAl_7)Al_4Si_{18}O_{69}(OH)_9$. Important substitutions like $F \rightarrow OH$, $Fe^{2+} \rightarrow Mg^{2+}$, $Fe^{3+} \rightarrow Al^{3+}$, and $(Mg + Fe^{2+} + Mn^{2+}) + Ti^{4+} \rightarrow 2\,(Al + Fe^{3+})$ have recently been studied and the corresponding local configurations have been discussed (Groat et al. 1992a, 1992b, 1994a, 1995; Fitzgerald et al. 1992; Ohkawa et al. 1992). Furthermore, the vesuvianite structure is able to accomplish up to 4 wt% B_2O_3 mainly by the coupled substitution $B + Mg \rightarrow 2H + Al$ (Groat et al. 1992a, 1994b, 1996, 1998).

The true symmetry of vesuvianite is under discussion. Transmission electron-microscopy of several samples show monoclinic symmetry combined with pseudomerohedral twinning (Veblen and Wiechmann 1991; Groat et al. 1993). Symmetry lower than tetragonal is also indicated by biaxial optical properties of many vesuvianites (Groat et al. 1993).

From a crystal chemical point of view, a simplified formula of vesuvianite may be written as $X_{18}X'Y_{12}Y'Z_{18}O_{69}(OH,F)_9$ where X and X' are sevenfold- to ninefold-coordinated, Y has octahedral coordination, Y' has square pyramidal coordination, and Z represents tetrahedral coordination. The positions X and X' are commonly occupied by Ca. The sites Y and Y' host elements with an average valence of 2.85 (e.g., 11 Al and 2 Mg) and Z is mainly occupied by Si.

Vesuvianites are commonly classified among orthosilicates (Deer et al. 1982) although the structure contains four disilicate units (Z3) in addition to ten SiO_4 orthosilicate groups (Z1 and Z2) per formula unit (pfu). The structure is closely related to that of grossular and mainly differs from that of garnet by the virtue of additional atoms (X' and Y') on the fourfold axes.

The vesuvianite structure exhibits channel-like arrangements along the fourfold axes. These channels are occupied by Y' and X' cations at various z levels. It is assumed that the Y' and X' periodicity is preserved within a single channel but adjacent channels may have Y' and X' at different z levels (e.g., Giuseppetti and Mazzi 1983; Fitzgerald et al. 1986b; Allen and Burnham 1992; Pavese et al. 1998; Armbruster and Gnos 2000). The different Y' and X' arrangements lead to various tetragonal space groups. Allen and Burnham (1992) provided strong arguments that ordered channel arrangements are favored in vesuvianites grown at low temperature (<300 °C). Such crystals exhibit either *P*4/*n* (centrosymmetric) or *P*4*nc* (acentric) space group symmetry. In addition, a macroscopic crystal may be assembled of domains representing both space groups. Thus the resulting symmetry becomes *P*4. Armbruster and Gnos (2000) discussed how the end-member polytypes can be distinguished based on diffraction experiments. Vesuvianites grown at high temperature (400–800 °C) exhibit long-range disordered channel arrangements and the resulting symmetry is *P*4/*nnc* (e.g., Allen and Burnham 1992).

*E-mail: armbruster@krist.unibe.ch

Vesuvianites occur in different colors which inspired Manning (1977) to present a loose classification in terms of color and transition-metal chemistry: (1) blue, pink, and lilac samples containing Cu^{2+}, Mn^{3+}, Cr^{3+}; (2) green vesuvianites in which Fe^{3+} is the main chromophore; (3) Fe^{2+} rich samples of brown or yellow color; (4) brown samples with mainly Fe^{2+} and Fe^{3+} in sites of unusual coordination. A modified color and chemical classification was also used by Fitzgerald et al. (1992).

The first detailed description of Mn-bearing vesuvianite was reported by Lasaulx (1883) from a serpentine massif in Lower Silesia (Poland). Orange-red crystals from this locality contained up to 3.2 wt% MnO. Dal Piaz et al. (1979) reported Mn-bearing vesuvianites with 2.45–2.85 wt% MnO from manganifereous deposits of the Valsesia-Valtournanche area (Italy). Groat et al. (1992a), performing a review of the chemistry of vesuvianites, reported MnO concentrations up to 3.8 wt% in samples from Långban, Sweden and up to 2 wt% in samples from Franklin, New Jersey. Fitzgerald et al. (1992) analyzed up to 3 wt% MnO in samples from Pajsberg, Sweden and in those from Franklin. Hålenius and Annersten (1994) investigated Mn-bearing vesuvianites (MnO > 2.4 wt%) from a skarn assemblage at Jacobsberg, Filipstad, Sweden. Cairncross at al. (1997) described a red Mn-rich (up to 5 wt% MnO) vesuvianite from the Kalahari manganese field (South Africa). The samples from Långban, Pajsberg, Jacobsberg, and Franklin, originate from manganese-rich skarn deposits whereas the Mn-rich vesuvianites from Lower Silesia are from rodingites in serpentinites. Vesuvianites from the Valsesia-Valtournanche area and from the Kalahari manganese fields are formed by hydrothermal alterations of Mn ores under rodingite-like conditions.

Hålenius and Annersten (1994) studied optical absorption spectra of Mn-bearing vesuvianites (with more than 1 Mn pfu) from Jacobsberg. The spectra showed one intense and strongly polarized band perpendicular to the *c* axis at 18000 cm^{-1} and a weak unpolarized band at 11500 cm^{-1}. The bands were assigned to a spin-allowed electronic d-d transition in Mn^{3+} at the five-fold-coordinated square pyramidal site (Y') and to a symmetry-forbidden d-d transition of Mn^{3+} at the same site, respectively. The high MnO concentration and the absence of additional Mn^{3+} characteristic absorptions suggested that surplus Mn (>1 Mn pfu) occurred in the divalent state. Platonov et al. (1995) recorded the absorption spectra of three color variants (lilac, yellow, and pink) of Mn-bearing vesuvianites with up to 1.1 wt% MnO from Lower Silesia. The lilac vesuvianites had the strongest band at 18500 cm^{-1} and the yellow vesuvianite the strongest absorption at 23600 cm^{-1}, both polarized perpendicular to the *c* axis. Pink samples were characterized by a superposition of bands found in the lilac and yellow crystals. In contrast to Hålenius and Annersten (1994), the 18500 cm^{-1} absorption of the lilac vesuvianites was preferentially assigned to Mn^{3+} ions in distorted octahedral coordination whereas the 23600 cm^{-1} absorption was attributed to Mn^{3+} in the five coordinated square-pyramids (Y'). Blue vesuvianites ("cyprine") have Jahn-Teller distorted Cu^{2+} in the square pyramidal Y'3 site (Fitzgerald et al. 1986a) and are characterized by a strong optical absorption perpendicular to the *c* axis at 15600 cm^{-1} (Dyrek et al. 1992).

During a systematic study of vein and pocket filling mineralizations from the Kalahari manganese fields (South Africa), we noticed dark lilac to purple rocks which were mainly composed of Mn-bearing grossular and vesuvianite with additional xonotlite, calcite, serandite, pectolite, strontiopiemontite, mozartite, and other rare manganese silicates. In this volume, Armbruster and Gnos (2000) report the first successful structure refinement of a low vesuvianite with *P*4*nc* symmetry from the N'chwaning II mine in the Kalahari manganese fields. Here we focus on the unusual crystal chemistry of Mn-rich vesuvianites.

EXPERIMENTAL METHODS

Three rock samples (NC1, NC9, and NC14) from the N'chwaning II mine, Kalahari manganese field (e.g., Cairncross et al. 1997) were studied. Vesuvianite comprised 3–80 vol% of the sample and occurred closely associated with grossular and pectolite-serandite. In addition to trace amounts of other Mn^{3+}-bearing minerals, including hydrogarnets (Al-substituted henritermierite), sample NC1 contained also 3–5 vol% strontiopiemontite and xonotlite.

All vesuvianite (001) cross-sections displayed very fine oscillatory color zoning where the color varied between different hues of lilac and orange (Fig. 1). Occasionally also sandglass like sectoring was observed at the crystal core if viewed with crossed polarizers. In thin sections perpendicular (001) these vesuvianites were colorless or exhibited a light yellow-brown or faint lilac hue. The crystals were optically negative characteristic of low-boron or boron-free vesuvianites (e.g., Groat et al. 1994b). The extreme zoning and small crystal size precluded that the average composition of vesuvianites selected for structural study could be determined. Thus the chemical variation was determined for larger areas in thin sections.

Minerals were analyzed on a Cameca SX-50 microprobe using beam conditions of 15kV and 20nA, wavelength-dispersive spectrometers, and when possible, an enlarged spot size of ca. 10 μm. Natural and synthetic minerals were used as standards: orthoclase Si*K*α (TAP) and K*K*α (PET), anorthite Al*K*α

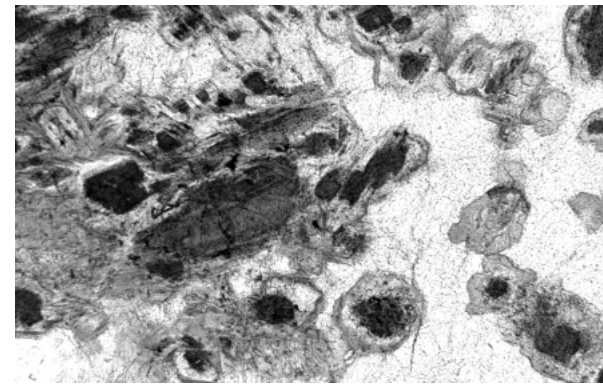

FIGURE 1. Thin section of strongly zoned Mn-bearing vesuvianite in a grossular (white) matrix (sample NC14). The dark red vesuvianite cores (dark gray) contain typically 6–9 wt% MnO, light lilac zones (light gray) and dark lilac rims (medium gray) contain 1.5–5 wt% MnO. Base of micrograph is 1 mm; recorded with plane polarized light.

(TAP) and Ca*K*α (PET), eskolaite Cr*K*α (LiF), almandine Fe*K*α (LiF), tephroite Mn*K*α (LiF), spinel Mg*K*α (TAP), covellite Cu*K*α (LiF), celestine Sr*L*α (PET), benitoite Ba*L*α (LiF), ilmenite Ti*K*α (LiF), albite Na*K*α (TAP), synthetic fluor phlogopite F*K*α (TAP), and scapolite Cl*K*α (PET). Data for Ba, Ti, F, and Cl were collected for 30 seconds, all other elements for 20 seconds. Pb, Zn, and Cr concentrations were found below detection limit in qualitative wavelength-dispersive scans, and hence were not analyzed further.

For selection of appropriate single-crystals for structural investigation a powder of samples NC1 and NC14 was produced. Several tiny crystals (<0.05 mm in their maximum dimension) were picked and studied by single-crystal X-ray methods using an Enraf Nonius CAD4 diffractometer (Mo*K*α-radiation) for the determination of the cell dimensions. If the X-ray reflections appeared sharp and oriented intergrowths of individual crystals could be excluded, a Siemens SMART three-circle diffractometer (Mo*K*α-radiation) equipped with a CCD detector was used for collection of intensity data. Special care was taken in measuring intensities of weak reflections because those are sensitive to the space group (either *P*4/*n* or *P*4*nc*) of low-temperature vesuvianites. Each frame was collected for 60 seconds with an ω-step width of 0.2°. Structure solution and refinement was carried out with the SHELX-97 program package (Sheldrick 1997) applying neutral atom scattering factors. Due to the similarity of Mn and Cu scattering factors the distribution of these transition metals could not be resolved. The same holds also for Al and Mg. As shown below the Mg and Cu concentrations are rather low in these vesuvianites. The atom numbering scheme was adopted from Pavese et al. (1998). Experimental details are in Table 1.

TABLE 1. CCD data collection and refinement of vesuvianite NC142 from N'chwaning II

Diffractometer	Siemens SMART CCD system
X-ray radiation	sealed tube Mo*K*α
X-ray power	50 kV, 40 mA
Temperature	293 K
Detector to sample distance	5.18 cm
Detector 2θ angle	27°
Resolution	0.77 Å
Rotation axis	ω
Rotation width	0.2°
Total number of frames	2810
Frame size	512 × 512 pixels
Data collection time per frame	60 s
Collection mode	hemisphere
Reflections measured	15496
max. 2θ	55.66; $-14 \le h \le 20$, $-20 \le k \le 18$, $-14 \le l \le 14$
Unique reflections	3190
Reflections > 2σ(I)	2832
Space group	*P*4/*n*, No. 85 (origin at $\bar{1}$)
Cell dimensions	a = 15.571(2), c = 11.789(2) Å
R(int)	3.9%
R(σ)	2.73%
Number of l.s. parameters	273
GooF	1.170
$R1$, $F_o > 4\sigma(F_o)$	3.85%
$R1$, all data	4.67%
$wR2$ (on F^2)	8.60%

$$R1 = \left(\Sigma \| F_o | - | F_c \| \right) / \left(\Sigma | F_o | \right)$$

$$wR2 = \sqrt{\left[\Sigma\left(F_o^2 - F_c^2\right)^2\right] / \left[\Sigma w \left(F_o^2\right)^2\right]}$$

$$\text{GooF} = \sqrt{\left[\Sigma\left(F_o^2 - F_c^2\right)^2\right] / (n-p)}$$

RESULTS

MnO is by far the dominant chromophore [Mn (Mn^{3+}) with concentrations up to 14.3 wt% (Table 2)]. Fe-contents are very low (considerably less than 1 wt% and mostly less than 0.1 wt%). Although many analyses show CuO concentration between 1 and 2 wt% the possible blue coloration (e.g., Fitzgerald et al. 1986a, 1992; Dyrek et al. 1992) seems completely overtoned by the color caused by Mn.

Crystal zones in vesuvianite containing 5–10 wt% MnO produce intense lilac to red color in (001) thin sections. Vesuvianites with MnO contents above ca. 10–12 wt% are orange-brownish in (001). MgO contents are generally below 2.5 wt% and mostly below 0.2 wt%. Strong variations were found in inversely correlated Al and (Mn + Cu + Ti + Mg + Fe) contents (Fig. 2). After Groat et al. (1992a), we normalized our analyses to 50 cations per formula unit (Table 2) and applied corresponding statistical tests. If the means of the distributions do not correspond to the number of sites, either some cations are wrongly assigned or the scheme of normalization is not correct. In addition, skew and kurtosis values should be low (kurtosis indicates too many data points in the tails of the distribution). The analyses were split into two groups containing > 2.4 wt% MnO (equivalent to ca 1 Mn pfu), and those with MnO concentrations < 2.4 wt% MnO (Fig. 3). In 32 vesuvianites with Mn contents above 1 Mn pfu the Si content is 17.85(16) apfu with skew and kurtosis values of –0.26 and –0.53. The Ca content is 19.02(14) apfu with skew and kurtosis values of 0.16 and –0.60. The histogram displaying the Si concentration of 72 vesuvianites with less than 1 Mn pfu exhibits a slightly bimodal distribution. The main maximum appears at 18.15 Si pfu and the second one at ca. 17.7 Si pfu. If the bimodal aspect is ignored a mean value of 18.01(26) Si pfu with skew and kurtosis values of –0.68 and –0.15 is obtained. The same data set yields 18.70(31) Ca pfu with skew and kurtosis values of 0.64 and –0.41. The distribution of X elements becomes more regular if also Na, K, Sr, and Ba are considered. Notice that especially Na becomes important for low-Mn vesuvianites. Adding Na, K, Sr and Ba as X site occupants of low-Mn vesuvianites increases the mean to 19.11(19) and reduces skew and kurtosis to –0.16 and –0.13. For the group with more than 1 Mn pfu a mean of 19.08(12) with skew 0.28 and kurtosis –0.34 is calculated.

All except one crystal (NC14-2) displayed weak but significant reflections which ruled out *P*4/*n* and *P*4*nc* symmetry thus space group *P*4 had to be assigned. However, due to strong correlations of atomic sites related by *P*4/*nnc* pseudo-symmetry, the results of the refinements were characterized by very high standard deviations of all variables. Thus it had to be assumed that such crystals are composed of *P*4/*n* and *P*4*nc* domains in various ratios and the *P*4 refinements had to be abandoned. As a compromise, structure refinements were carried out in the long-range disordered space group *P*4/*nnc* where the *n*- and *c*-glide violating reflection had to be disregarded. Corresponding refinements provide information on the distribution of Mn on Y and

TABLE 2. Representative electron microprobe analyses of manganese vesuvianites from the N'chwaning II mine of the Kalahari manganese field

	NC9-1	NC9-4	NC9-7	NC9-22	NC14-49	NC14-41	NC14-3	NC14-38	NC1-7	NC1-12	NC14-18	NC14-16
SiO_2	37.28	36.59	35.03	35.91	36.35	36.91	35.52	34.13	36.46	35.44	36.40	35.37
TiO_2	0.00	0.00	0.00	0.00	0.01	0.00	0.06	0.00	0.00	0.00	0.00	0.00
Al_2O_3	19.93	18.33	13.55	15.72	17.99	19.33	15.77	10.63	20.76	19.32	17.01	14.92
FeO	0.01	0.01	0.07	0.00	0.56	0.38	0.00	0.00	0.02	0.00	0.00	0.06
MnO	1.91	4.22	10.80	8.09	2.11	3.33	8.61	14.34	0.53	2.93	6.85	9.35
MgO	0.00	0.07	0.02	0.00	1.82	0.18	0.11	0.09	0.35	0.01	0.01	0.00
CaO	35.83	35.79	34.68	35.00	36.13	35.26	35.24	34.33	35.16	35.05	35.31	35.09
CuO	0.98	1.14	0.00	0.22	0.69	0.37	0.00	0.41	2.39	1.59	0.10	0.13
SrO	0.04	0.06	0.11	0.13	0.13	0.20	0.14	0.05	0.00	0.00	0.20	0.22
BaO	0.00	0.00	0.01	0.00	0.04	0.08	0.05	0.00	0.00	0.00	0.00	0.00
Na_2O	0.48	0.16	0.07	0.15	0.03	0.45	0.03	0.00	0.72	0.69	0.14	0.14
K_2O	0.00	0.00	0.00	0.01	0.00	0.00	0.00	0.01	0.00	0.00	0.00	0.00
F	0.22	0.26	0.19	0.24	0.24	0.08	0.11	0.12	0.53	0.33	0.26	0.26
Cl	0.01	0.01	0.00	0.00	0.00	0.00	0.00	0.00	0.01	0.01	0.00	0.00
Total	96.69	96.64	94.53	95.47	96.10	96.57	95.64	94.11	96.93	95.37	96.28	95.54
Si	18.190	18.038	17.945	18.077	17.837	18.063	17.846	17.761	17.739	17.579	18.100	17.859
Ti	0.000	0.000	0.000	0.000	0.002	0.000	0.021	0.000	0.000	0.000	0.000	0.000
Al	11.460	10.649	8.181	9.325	10.405	11.149	9.338	6.522	11.905	11.295	9.971	8.881
FeII	0.005	0.005	0.032	0.000	0.230	0.156	0.000	0.000	0.008	0.000	0.000	0.024
MnII	0.789	1.760	4.686	3.447	0.875	1.382	3.666	6.321	0.217	1.230	2.884	3.998
Mg	0.000	0.049	0.018	0.000	1.328	0.133	0.084	0.073	0.254	0.007	0.005	0.001
Ca	18.732	18.904	19.038	18.876	18.995	18.485	18.969	19.139	18.326	18.624	18.811	18.983
Cu	0.361	0.425	0.000	0.082	0.256	0.136	0.000	0.160	0.877	0.595	0.037	0.051
Sr	0.011	0.017	0.032	0.037	0.038	0.056	0.040	0.014	0.000	0.000	0.058	0.064
Ba	0.000	0.000	0.002	0.000	0.008	0.015	0.011	0.000	0.000	0.000	0.000	0.000
Na	0.451	0.153	0.066	0.150	0.026	0.426	0.025	0.000	0.675	0.666	0.133	0.140
K	0.000	0.000	0.000	0.007	0.000	0.000	0.000	0.009	0.000	0.003	0.002	0.000
F	0.344	0.404	0.308	0.377	0.379	0.132	0.181	0.193	0.819	0.524	0.403	0.422
Cl	0.008	0.010	0.002	0.003	0.000	0.000	0.000	0.000	0.007	0.004	0.000	0.000
Σcat	50.000	50.000	50.000	50.000	50.000	50.000	50.000	50.000	50.000	50.000	50.000	50.000

Notes: Chemical formulae normalized to 50 cations.

Y' sites. Reflection intensities of crystal NC14-2 indicated the predominance of *P*4/*n* long-range ordering.

Atomic coordinates and populations of crystal NC14-2 are given in Table 3, anisotropic displacement parameters in Table 4[1], and selected interatomic distances in Table 5 (deposited). Detailed results of the average *P*4/*nnc* refinements of the other crystals are not tabulated and not considered further but the most important findings (Table 6) are used to support the results of the *P*4/*n* refinement of crystal NC14-2. The latter crystal had 75% of Y' and X' cations arranged in a type A string with the remaining 25% in a type B string. The structure refinement converged to a 1/1 merohedral {110} twin. Surprisingly, mean Si-O distances for the sites Si1a, Si1b, and Si2a were 1.659, 1.670, and 1.654 Å, respectively. These distances are significantly longer than in any other vesuvianites hitherto structurally investigated (see Fig. 6 of Groat et al. 1992a). In addition, difference-Fourier maps revealed negative peaks on these Si sites indicating that the corresponding populations were overestimated. In subsequent refinement cycles the isotropic displacement parameter of all Si sites were constrained to a common value and the populations of Si1a, Si1b, Si2a, and Si2b were allowed to vary. Constraints on displacement parameters were introduced to reduce correlation effects between population and atomic displacement. Population refinements yielded significant vacancies (9–17%) on just those Si sites for which increased mean Si-O bond distances were calculated.

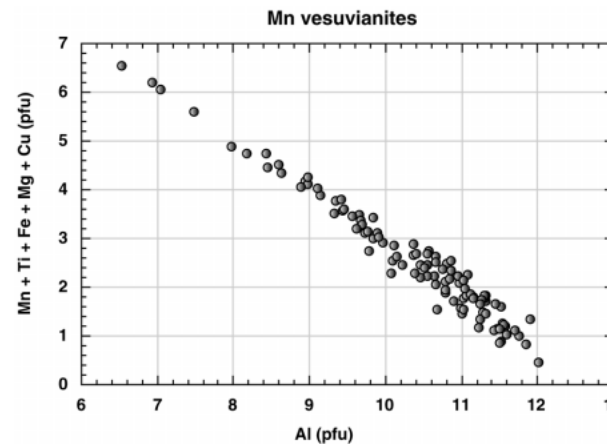

FIGURE 2. Negative correlation among Y-type cations in vesuvianites from the N'chwaning mine (Kalahari manganese fields) determined by electron-microprobe analyses. The error of each data point (based on counting statistics and multiple determinations) is significantly below the size of the symbol. In an idealized stoichiometric vesuvianite there are 13 Y-type cations pfu and the average valence of Y is 2.85. If we neglect the contribution by Ti^{4+} (< 0.02 apfu) there are eleven Y^{3+} and two Y^{2+}. The dominant cation (Table 2) replacing Al is Mn. Incorporation of Mn^{3+} is required for (Mn + Ti + Fe + Mg + Cu) concentrations > 2 apfu.

[1]For a copy of Tables 4 and 5, document item AM-00-037, contact the Business Office of the Mineralogical Society of America (see inside front cover of recent issue) for price information. Deposit items may also be available on the American Mineralogist web site (http://www.minsocam.org or current web address).

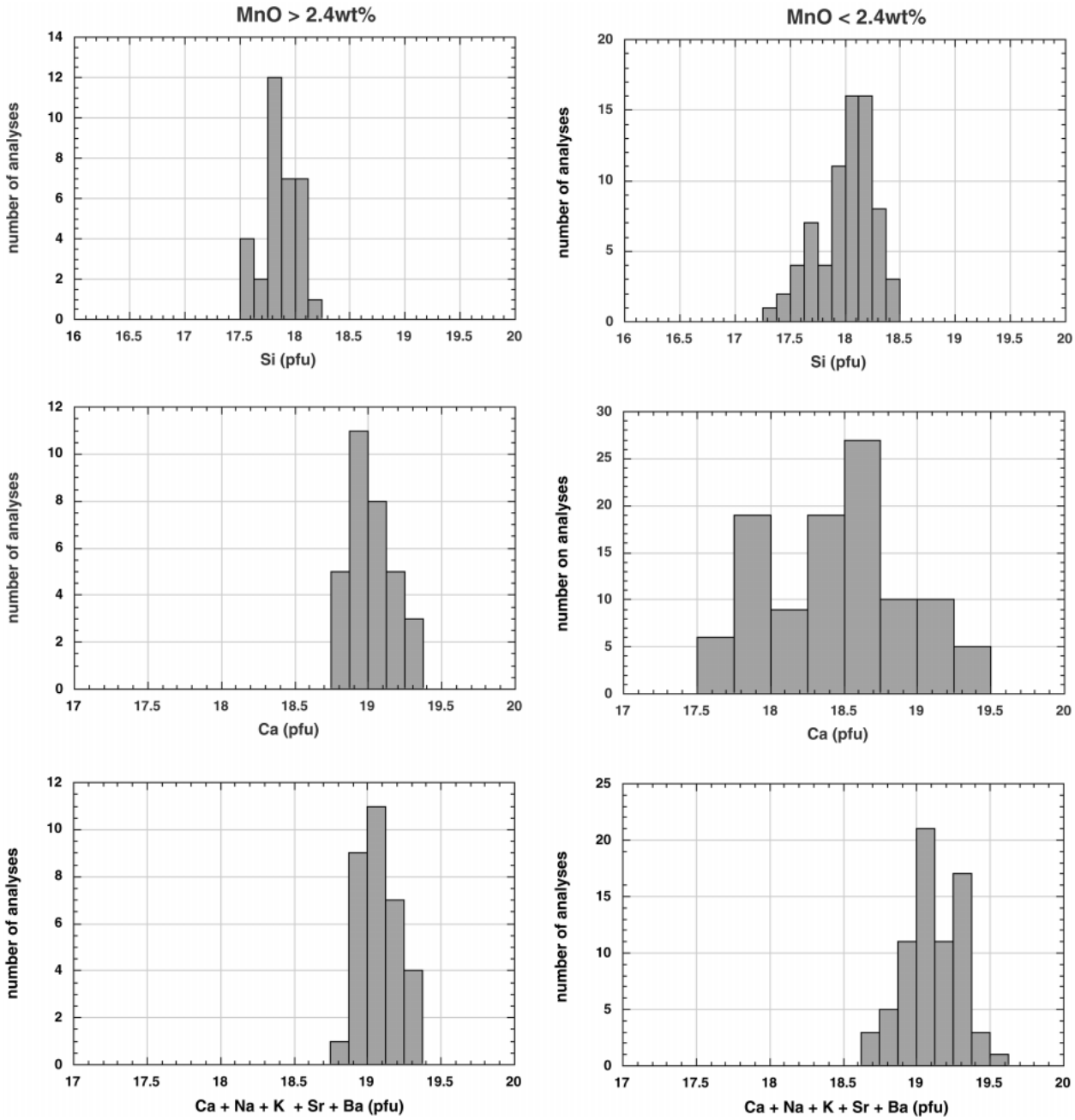

FIGURE 3. Left column: histogram of Si (pfu) and Ca (pfu) abundances for 32 vesuvianite analyses with MnO > 2.4 wt% (Mn > 1 apfu). Mean, skew and kurtosis for Si are 17.85(16) apfu, –0.26, and –0.53. Corresponding values for Ca are 19.02(14) apfu, 0.16, and –0.60, respectively. Right column: histograms for 72 vesuvianite analyses with MnO < 2.4 wt% (Mn < 2 apfu). Mean, skew and kurtosis for Si are 18.01(26) apfu, –0.68, and –0.15. Corresponding values for Ca are 18.70(31) apfu, 0.64 and –0.41, respectively. Notice that the spreading of X cations is reduced if (Ca + Na + K + Sr + Ba) is considered.

Considering the site multiplicities of the various tetrahedral sites 17.37(5) Si pfu were located which significantly deviates from the ideal composition with 18 Si pfu. Vacancies were only found in orthosilicate groups of type Z1 and Z2 but not in the disilicate units of type Z3. Corresponding results were also found for several crystals refined in space group *P*4/*nnc* (Table 6). However, also Mn-poor crystals with "normal" Si-O distances and without any indication of tetrahedral vacancies were detected (e.g., Table 6, and Armbruster and Gnos 2000). Qualitatively, vacancies on Si sites (Z1, Z2) were more pronounced for Mn-rich samples. Mn strongly prefers the Y' site followed by Y2 and Y1. In the *P*4/*n* refinement there is also a strong Mn parti-

TABLE 3. Final atomic coordinates and B_{eq} (Å^3) values for vesuvianite NC14-2 in space group *P4/n* (origin at $\bar{1}$)

atom	population	*x/a*	*y/b*	*z/c*	B_{eq}
Si1a	0.91(1) Si	–¼	¼	0	0.55(1)*
Si1b	0.83(1) Si	–¼	¼	½	0.55(1)*
Si2a	0.908(6) Si	–0.0407(2)	0.3184(2)	0.1305(2)	0.55(1)*
Si2b	0.992(6) Si	–0.0418(1)	0.1804(1)	0.3720(2)	0.55(1)*
Si3a		0.0875(1)	0.3483(1)	–0.1352(2)	0.55(1)*
Si3b		0.0805(1)	0.1507(1)	0.6350(2)	0.55(1)*
Al1a	0.22(1) Mn + 0.78 Al	0	0	0	0.51(5)*
Al1b	0.08(1) Mn + 0.92 Al	–½	0	½	0.45(6)*
Al2a	0.35(1) Mn + 0.65 Al	–0.1111(1)	0.1177(1)	0.1249(1)	0.54(4)*
Al2b	0.13(1) Mn + 0.87 Al	–0.3889(1)	0.1204(1)	0.3739(1)	0.53(4)*
Ca1		–¼	¼	0.2513(2)	0.68(2)
Ca2a		–0.0446(1)	0.1882(1)	–0.1202(1)	0.74(3)
Ca2b		0.1892(1)	–0.0419(1)	0.6219(1)	0.69(3)
Ca3a		0.0975(1)	0.1778(1)	0.1176(1)	1.33(3)
Ca3b		–0.3984(1)	–0.1809(1)	–0.3906(1)	1.13(3)
O1a		–0.2199(3)	0.1721(3)	0.0873(4)	0.63(8)
O1b		–0.2825(3)	0.1712(4)	0.4140(4)	0.96(9)
O2a		–0.1179(4)	0.3378(3)	0.2243(4)	0.65(8)
O2b		–0.1178(4)	0.1571(3)	0.2808(4)	0.90(8)
O3a		–0.0489(3)	0.2210(3)	0.0756(4)	0.90(9)
O3b		–0.0499(3)	0.2772(3)	0.4252(4)	0.58(8)
O4a		–0.0624(3)	0.3925(3)	0.0314(4)	0.89(9)
O4b		–0.0641(3)	0.1061(3)	0.4714(4)	0.84(9)
O5a		–0.0102(3)	0.3268(3)	–0.1760(4)	0.90(9)
O5b		–0.0167(3)	0.1685(3)	0.6800(4)	1.04(9)
O6a		0.1231(4)	0.2712(3)	–0.0574(4)	1.2(1)
O6b		0.1159(4)	0.2293(3)	0.5602(4)	1.15(9)
O7a		0.0556(3)	0.3256(3)	0.1821(4)	1.12(9)
O7b		0.0552(3)	0.1734(3)	0.3258(4)	1.1(1)
O8a		0.0929(3)	0.4378(3)	–0.0655(4)	0.65(8)
O8b		0.0904(3)	0.0608(3)	0.5674(4)	0.85(9)
O9		0.1489(4)	0.3582(4)	–0.2504(4)	0.82(9)
O10a		¼	¼	0.1332(8)	1.9(2)
O10b		–¼	–¼	–0.3558(9)	1.9(1)
O11a		–0.0059(3)	0.0607(3)	0.1367(4)	0.72(9)
O11b		–0.4943(3)	0.0634(3)	0.3635(4)	0.80(8)
CaX'4b	0.253(6) Ca	¼	¼	–0.1469(9)	0.7(2)*
MnY'3b	0.253(6) Mn	¼	¼	0.5470(9)	2.2(2)*
CaX'4a	0.747(6) Ca	¼	¼	0.6470(3)	1.01(5)
MnY'3a	0.747(6) Mn	¼	¼	–0.0441(3)	1.17(4)
O12a	0.06(1) O	0.143(4)	0.292(4)	0.214(5)	0.79*
O12b	0.04(1) O	0.161(6)	0.227(5)	0.293(7)	0.79*
T2	0.12(1) B	–0.253(6)	–0.222(2)	–0.228(2)	0.79*

* Isotropically refined.

TABLE 6. Selected structural parameters of Mn-bearing vesuvianites from the N'chwaning II mine refined in space group *P4/nnc*

sample	NC14-2 *P4/n* (avg)	NC14-1 *P4/nnc*	NC14-4 *P4/nnc*	NC1-2 *P4/nnc*	NC1-1 *P4/nnc*	NC1-4 *P4/nnc*
a (Å)	15.571(2)	15.508(2)	15.599(3)	15.511(2)	15.514(1)	15.502(3)
c (Å)	11.789(2)	11.780(3)	11.805(4)	11.778(3)	11.772(3)	11.782(4)
Pop. Z1	0.87(1)	0.918(6)	0.86(2)	1.0	0.92(1)	1.0
<Z1-O> (Å)	1.665	1.653	1.664	1.633	1.645	1.634
Pop. Z2	0.95(1)	0.95(1)	0.95(2)	1.0	0.96(1)	1.0
<Z2-O> (Å)	1.648	1.644	1.646	1.645	1.646	1.642
Pop. Y1	0.85(1) Al + 0.15 Mn	1.0 Al	0.89(2) Al + 0.11 Mn	1.0 Al	1.0 Al	1.0 Al
<Y1-O> (Å)	1.912	1.897	1.913	1.901	1.898	1.899
Pop. Y2	0.76(1) Al + 0.24 Mn	0.94(1) Al + 0.06 Mn	0.77(1) Al + 0.23 Mn	0.89(1) Al + 0.11 Mn	0.89(1) Al + 0.11 Mn	0.88(1) Al + 0.12 Mn
<Y2-O> (Å)	1.947	1.932	1.957	1.939	1.937	1.939
Pop. Y'3	0.5 Mn	0.12(1) Mn + 0.38 Al	0.45(2) Mn + 0.05 Al	0.42(2) Mn + 0.08 Al	0.25(1) Mn + 0.25Al	0.50 Mn

tion between a- and b-suffixed sites. The a-suffixed sites have by a factor of three more Mn than the corresponding b-suffixed sites. Increased Mn on octahedral sites is also reflected in increased mean Y-O distances. Very weak electron density peaks in difference Fourier maps yielded T2 and O12a and O12b sites which Groat et al. (1996) assigned to additional boron (T2) and coordinating O sites (O12a and O12b). The O12 sites are close (<2 Å) to O7 and O10 sites thus vacancies have to be assumed on O7 and O10 positions if O12 sites are occupied. However the low occupation of O12 positions (ca. 5%) did not allow vacancy refinement on the adjacent O sites. The refined electron density on T2 may be interpreted in terms that the crystal contained ca. 0.5 B pfu. Notice that the electron density at T2 is below 1 e/Å^3. Thus without the detection of the low occupied O12 sites T2 could also be interpreted as a disordered H position forming an OH group with O10a (Groat et al. 1994a).

DISCUSSION

In previous structure refinements, Si1-O distances were reported in the range between 1.63 and 1.64 Å and the mean Si2-O distances were slightly larger with 1.64 to 1.65 Å. However, Si1a-O and Si1b-O distances of 1.66 and 1.67 Å as found in the Mn-rich vesuvianite NC14-2, respectively, have not been reported for vesuvianites before (see Fig. 6 of Groat et al. 1992a). Increased Si-O distances may occur due to substitution of Si by Al but Al has a very similar scattering power for X-rays as Si and such a substitution cannot explain the reduced electron density at the Si sites. Other potential tetrahedral cations with low X-ray scattering power such as Be and B do not have ionic radii larger than Si which could explain an increase of mean Si-O distances. In garnets formed at low temperature, the so-called hydrogarnet substitution is well established where a SiO_4 unit may locally be replaced by an H_4O_4 tetrahedron. The latter tetrahedron has a vacant center and the protons are positioned slightly above the tetrahedral faces. The distance between the tetrahedron center and the surrounding O sites is ca. 1.96–1.98 Å (Lager et al. 1987; Armbruster et al. in preparation). Hydrogarnets like henritermierite and hydrous andradite are also known from fissure and pocket fillings in the N'chwaning II mine. The structural similarity between vesuvianite and garnet suggests that a hydrogarnet-type substitution could also exist in vesuvianite (Lager et al. 1999).

The analytical data of Mn-bearing vesuvianites displayed in Figure 3 suggest, though at the edge of significance, that other elements than Si occupy the tetrahedral Z sites. For Mn-rich vesuvianites the mean is slightly lower than 18 Si pfu and for Mn-poor vesuvianites the distribution is skewed toward lower values. Both observations are in agreement with the Si deficit on Z1 and Z2 sites derived from the structure refinements.

IR spectroscopic evidence of a hydrogarnet-like substitution is difficult to establish because vesuvianites show OH stretching bands over a wide range between 3700 and 3000 cm^{-1}. Groat et al. (1995) identified twelve OH-related absorptions due different local cation and anion configurations. In the Mn^{3+} hydrogarnet henritermierite each Mn^{3+} octahedron is linked to two O_4H_4 tetrahedra which enhances the Mn^{3+} Jahn-Teller distortion by development of hydrogen bonds (Armbruster et al. in prep.). A corresponding simple relation was not found for the NC14-2 vesuvianite. The octahedron Y2a with the highest Mn substitution (35%) is not connected to Si1b with the highest vacancy concentration but the octahedron Y1b with the lowest Mn substitution (8%) is bonded twice to Si2b without significant vacancies. The octahedral bonding environment in vesuvianite is much more complex than in garnets because in vesuvianite Y1 octahedra have one and Y2 octahedra have two OH groups (O11 sites) without an assumed additional hydrogarnet-like substitution. Furthermore, a typical Jahn-Teller distortion cannot be identified for Y2a with the highest Mn substitution. This suggests that the partially ordered arrangement of empty and Si centered tetrahedra is favored for strain reduction caused by the partially ordered substitution of Mn.

A comparison of Y'3a-O distances for the square pyramidal site can only be made for long-range ordered vesuvianites because in disordered *P*4/*nnc* structures a corresponding Y'3 site is only 50% occupied and the Y'3-O distances are average distances of vacancies and occupied sites both surrounded by O sites. All low-symmetry (*P*4/*n* and *P*4*nc*) vesuvianites hitherto studied by diffraction methods have a partly disordered string arrangement parallel to the fourfold axes where one string type is dominated by ca. 80% (e.g., Pavese et al. 1998; Armbruster and Gnos 2000). As a consequence, this partial disorder gives rise to increased mean bond-distances between Y'3 and O.

In the *P*4/*n* crystal from Asbestos studied by Fitzgerald et al. (1986b) the mean Y'3-O distance (their occupied B site) was 1.873 Å and Al^{3+} was assumed in fivefold coordination (Phillips et al. 1987). A corresponding bond-valence calculated Al-O distance (Brown 1997) is 1.809 Å. A different Asbestos crystal studied by Armbruster and Gnos (2000) had Fe^{3+} on Y'3a with mean Y'3a-O of 1.972 Å. Pavese et al. (1998) determined Fe^{3+} on M3a for an Italian vesuvianite yielding a corresponding mean Y'3-O distance of 1.976 (X-ray data) and 2.043 Å (neutron data) whereas bond valence calculations would suggest 1.948 Å. Crystal NC14-4 (this study) gave a mean Y'3a-O distance of 2.025 Å which is considerably longer than expected for Mn^{3+} but shorter than expected for Mn^{2+}. Based on bond-valence calculations fivefold-coordinated Mn^{2+} should yield an average Mn-O bond length of 2.13 Å, whereas Mn^{3+} should yield 1.95 Å. Furthermore, for Mn^{3+} in fivefold coordination one would expect a characteristic Jahn-Teller distortion such that the bond perpendicular to the square base is either elongated or shortened. This elongation is only weakly developed with Y3a-O10a of 2.09 Å whereas $4 \times$ Y'3a-O6a is 2.01 Å. In contrast, the *P*4*nc* vesuvianite from the N'chwaning mine studied by Armbruster and Gnos (2000) had Y'3a-O10a of 2.33 Å and $4 \times$ Y'3a-O6a of 2.00 Å with mainly the Jahn-Teller ions Cu^{2+} and Mn^{3+} occupying Y'3a. This suggests that in crystal NC14-2 (this study) Mn^{2+} and Mn^{3+} are occupying Y'3a in a disordered fashion. This disorder may also be responsible for the various lilac to orange-red hues (Platonov et al. 1995) seen in (001) thin sections of vesuvianites from the N'chwaning mine.

Crystal NC14-4 in Table 6 has the largest cell dimensions and also the longest mean <Y2-O> distance (1.957 Å). However, the structure refinement yielded the same Mn concentration (23%) on Y2 as for crystal NC14-2 for which a mean <Y2-O> distance of 1.947 Å was obtained. This may indicate the mixed valence (Mn^{2+}, Mn^{3+}) character where increased Mn^{2+} concentrations relative to Mn^{3+} cause octahedral expansion and in turn increased cell dimensions. Our observation that vesuvianites with the highest measured MnO concentrations exhibit orange-brownish color may support the absorption band assignment by Hålenius and Annersten (1994) who suggested that the lilac color is due to Mn^{3+} in square pyramidal (Y'3) coordination. For stoichiometric reasons increasing MnO content must lead to more Mn^{3+} occupied octahedral sites enhancing absorptions described by Platonov et al. (1995) for yellow Mn-bearing vesuvianite at 23 600 cm^{-1}. Thus increased contribution of this absorption type leads to the observed orange-brownish colors for Mn-rich samples.

REFERENCES CITED

Allen, F.M. and Burnham, C.W. (1992) A comprehensive structure-model for vesuvianite: Symmetry variations and crystal growth. Canadian Mineralogist, 30, 1–18.

Armbruster, T. and Gnos, E. (2000) *P4/n* and *P4nc* long-range ordering in low-temperature vesuvianites. American Mineralogist, 85, 563–569.

Brown, I.D. (1996) VALENCE: a program for calculating bond valences. Journal of Applied Crystallography, 29, 479–480.

Cairncross, B., Beukes, N., and Gutzmer, J. (1997) The Manganese Adventure; The South African Manganese Fields. Associated Ore and Metal Cooperation Limited. Marshalltown, Johannesburg 2107, Rebublic of South Africa, 236 p.

Dal Piaz, G.V., Di Battistini, G., Kienast, J.R., and Venturelli, G. (1979) Manganiferous quarzitic schists of the Piemonte ophiolite nappe in the Valsesia-Valtournanche area (Italian Western Alps). Memorie di Scienze Geologiche, 32, 4–22.

Deer, W.A., Howie, R.A., and Zussman, J. (1982) Rock-forming Minerals, Vol. 1A, second Edition, 919 p. Orthosilicates, Longman, London.

Dyrek, K., Platonov, A.N., Sojka, Z., and Zabinski, W. (1992) Optical absorption and EPR study of Cu^{2+} ions in vesuvianite ("cyprine") from Sauland, Telemark, Norway. European Journal of Mineralogy, 4, 1285–1289.

Fitzgerald, S., Rheingold, A.L., and Leavens, P.B. (1986a) Crystal structure of a Cu-bearing vesuvianite. American Mineralogist, 71, 1011–1014.

——(1986b) Crystal structure of a non-*P4/nnc* vesuvianite from Asbestos, Quebec. American Mineralogist, 71, 1483–1488.

Fitzgerald, S., Leavens, P.B., and Nelen, J.A. (1992) Chemical variation of vesuvianite. Mineralogy and Petrology, 46, 163–178.

Giuseppetti, G. and Mazzi, F. (1983) The crystal structure of a vesuvianite with *P4/n* symmetry. Tschermaks Mineralogische und Petrographische Mitteilungen, 31, 277–288.

Groat, L.A., Hawthorne, F.C., and Ercit, T.S. (1992a) The chemistry of vesuvianite. Canadian Mineralogist, 30, 19–48.

——(1992b) The role of fluorine in vesuvianite: A crystal-structure study. Canadian Mineralogist, 30, 1065–1075.

Groat, L.A., Hawthorne, F.C., Ercit, T.S., and Putnis, A. (1993) The symmetry of vesuvianite. Canadian Mineralogist, 31, 617–635.

Groat, L.A., Hawthorne, F.C., and Ercit, T.S. (1994a) Excess *Y*-group cations in the crystal structure of vesuvianite. Canadian Mineralogist, 32, 497–504.

——(1994b) The incorporation of boron into the vesuvianite structure. Canadian Mineralogist, 32, 505–523.

Groat, L.A., Hawthorne, F.C., Rossman, G.R., and Ercit, T.S. (1995) The infrared spectroscopy of vesuvianite in the OH region. Canadian Mineralogist, 33, 609–626.

Groat, L.A., Hawthorne, F.C., Lager, G.A., Schultz, A.J., and Ercit, T.S. (1996) X-ray and neutron crystal structure refinements of a boron-bearing vesuvianite. Canadian Mineralogist, 34, 1059–1070.

Groat, L.A., Hawthorne, F.C. Ercit, T.S., and Grice, J.D. (1998) Wiluite, $Ca_{19}(Al,Mg,Fe,Ti)_{13}(B,Al)_5Si_{18}O_{68}(O,OH)_{10}$, a new mineral species isostructural with vesuvianite, from the Sakha Republic, Russian Federation. Canadian Mineralogist, 36, 1301–1304.

Hålenius, U. and Annersten, H. (1994). Five-coordinated trivalent manganese in vesuvianite: A spectroscopic study. International Mineralogical Association, 16th General Meeting, Pisa, Italy, 162–163.

Lager, G.A., Armbruster, T., and Faber, F. (1987) Neutron and X-ray diffraction study of hydrogarnet $Ca_3Al_2(O_4H_4)_3$. American Mineralogist, 72, 756–765.

Lager, G.A., Xie, Q., Ross, F.K., Rossman, G.R., Armbruster, Th., Rotella, F.J., and Schultz, A.J. (1999) Hydrogen-atom positions in P4/nnc vesuvianite. Canadian Mineralogist, 37, 763–768.

Lasaulx, von A. (1883) ber den Manganvesuvian vom Johnsberge bei Jordansmühle in Schlesien und Über den Titanomorphit. Zeitschrift für Kristallographie und Mineralogie, 7, 71–73.

Manning, P.G. (1977) Charge-transfer interactions and the origin of colour in brown vesuvianites. Canadian Mineralogist, 15, 508–511.

Ohkawa, M., Yoshiasa, A., and Takeno, S. (1992) Crystal chemistry of vesuvianite: Site preferences of square-pyramidal coordinated sites. American Mineralogist, 77, 945–953.

Pavese, A., Prencipe, M., Tribaudino, M., and Aagaard, St.S. (1998) X-ray and neutron single-crystal study of *P4/n* vesuvianite. Canadian Mineralogist, 36, 1029–1037.

Phillips, B.L., Allen, F.M., and Kirkpatrick, R.J. (1987) High-resolution solid-state ^{27}Al NMR spectroscopy of Mg-rich vesuvianite. American Mineralogist, 72, 1190–1194.

Platonov, A.N., Zabinski, W., and Sachanbinski, M. (1995) Optical absorption spectra of Mn^{3+} ions in vesuvianites from Lower Silesia, Poland. European Journal of Mineralogy, 7, 1345–1352.

Sheldrick, G.M. (1997) SHELX-97, program for crystal structure determination, University of Göttingen, Germany.

Valley, J.W., Peacor, D.R., Bowman, J.R., Essene, E.J., and Allard, M.J. (1985) Crystal chemistry of a Mg-vesuvianite and implications of phase equilibria in the system $CaO\text{-}MgO\text{-}Al_2O_3\text{-}SiO_2\text{-}H_2O\text{-}CO_2$. Journal of Metamorphic Geology, 3, 137–153.

Veblen, D.R. and Wiechmann, M.J. (1991) Domain structure of low-symmetry vesuvianite from Crestmore, California. American Mineralogist, 76, 397–404.

MANUSCRIPT RECEIVED JUNE 8, 1999
MANUSCRIPT ACCEPTED OCTOBER 20, 1999
PAPER HANDLED BY JOHN RAKOVAN